

INVESTIGATING iASPP AS A POTENTIAL CANCER DRUG TARGET

By

Laura Keigher

Thesis

Submitted to the Faculty of the  
Graduate School of Vanderbilt University  
in partial fulfillment of the requirements

for the degree of

MASTER OF SCIENCE

in

Chemical and Physical Biology

December, 2012

Nashville, TN

Approved:

Dr. Stephen Fesik

Dr. Charles Sanders

Dr. David Piston

## Acknowledgements

First, I would like to thank my mentor, Dr. Stephen Fesik, for his continued guidance and support throughout my graduate career. His constant guidance and motivation through difficult aspects of research are forever appreciated. He is a learned and inventive scientist for whom I am grateful to have studied under. He is an inspiration to young scientists everywhere.

The Chemical and Physical Biology Department as a whole has been extremely supportive throughout my graduate career. I could not have done any of this work without the guidance of Dr. Hassane Mchaourab and my committee members, Dr. Dave Piston and Dr. Chuck Sanders. I will always appreciate their time and advice throughout my graduate studies.

I will be forever indebted to Dr. Olivia Rossanese, Dr. Ed Olejniczak, and Dr. Jason Phan for their constant guidance in the laboratory and beyond. It was only with their support and immeasurable knowledge that I was able to pursue these research efforts.

I would also like to thank fellow graduate students for their support on difficult aspects of this project, Craig Goodwin and Michael Burns. Dr. Dominico Vigil is a talented scientist and postdoctoral fellow of the lab and I would like to thank him for his guidance in my assay development.

## Table of Contents

Acknowledgements.....	ii
List of Figures.....	iv
List of Tables.....	v
Chapter	
I. Introduction.....	1
II. Preparation of iASPP for fragment-based screening.....	9
Introduction.....	9
Methods.....	9
Results.....	11
III. Fragment-based screen.....	23
Introduction.....	23
Experimental Design.....	24
Methods.....	26
Results.....	27
IV. Assay Development.....	39
Introduction.....	39
Experimental Design.....	39
Methods.....	42
Results.....	42
V. Summary.....	53
References.....	55

## List of Figures

Figure	Page
1. Domains of ASPP protein family.....	2
2. Structural Similarity of ASPP family members.....	2
3. Abbreviated p53/p73 pathway.....	6
4. SOFAST-HMQC spectrum of iASPP $\Delta$ 623-828.....	13
5. SOFAST-HMQC spectrum of iASPP $\Delta$ 608-825.....	20
6. SOFAST-HMQC spectra of iASPP free and bound to GSPRKARRA.....	21
7. SOFAST-HMQC spectra of iASPP free and bound to p-53 linker.....	22
8. NMR fragment-based screen approach.....	25
9. SOFAST-HMQC spectra of iASPP free and bound to a fragment.....	28
10. FPA assay.....	41
11. NMR titration of 9 mer labeled with FITC and unlabeled.....	45
12. FPA assay titration of 9 mer.....	46
13. FPA assay binding curve with addition of detergents.....	47
14. Curve of unlabeled 9 mer off competing labeled 9 mer.....	48
15. Total fluorescence as a function of iASPP concentration.....	49
16. Total fluorescence when unlabeled 9 mer off competes labeled 9 mer.....	50

## List of Tables

Table	Page
1. Diazapene compounds.....	30
2. Quinoline compounds with 2-ring structure.....	32
3. Quinoline compounds with 3-ring structure.....	34
4. Amino-benzimidazole compounds.....	35
5. compounds similar to amino-benzimidazole series.....	36
6. Peptide sequences investigated for use in FPA assay.....	44

## CHAPTER I

### INTRODUCTION

iASPP is the inhibitory member of the ASPP family. The ASPP family of proteins are named for both their structure (ankyrin repeats, SH3 domain, proline rich protein) and function (apoptosis stimulating protein of p53) (Ahn et al. 2009; Robinson et al. 2008). Figure 1 illustrates the domains present in the ASPP family and their relative position in the ASPP protein family members. There are three members of the ASPP family: iASPP, which is anti-apoptotic, ASPP2, which is considered to be pro-apoptotic, and ASPP1, which has been shown to exhibit apoptotic effects in the nucleus while producing anti-apoptotic effects when present in the cytoplasm (Vigneron et al. 2010; Bergnamaschi et al. 2003). iASPP binds to and prevents p53 and p73 from transactivating their pro-apoptotic targets while nuclear ASPP1 and ASPP2 bind to p53 and p73 and assist transactivation of target genes (Ahn et al. 2009; Robinson et al. 2008; Sullivan et al. 2007). Despite their structural similarities (Figure 2), data suggest that iASPP and ASPP2 bind to p53 at different sites (Ahn et al. 2009). ASPP2 binds to the core domain of p53; whereas, the evidence suggests that iASPP binds to the linker region of p53 (Ahn et al. 2009). It has also been suggested that iASPP may bind to and inhibit the ASPP2-p53 complex (Ahn et al. 2009). Specifically, it is the C-terminal region of iASPP that is responsible for its anti-apoptotic effects (Robinson et al. 2008; Ahn et al. 2009). However, it is unknown which residues of the p53 linker region are necessary for binding to iASPP.

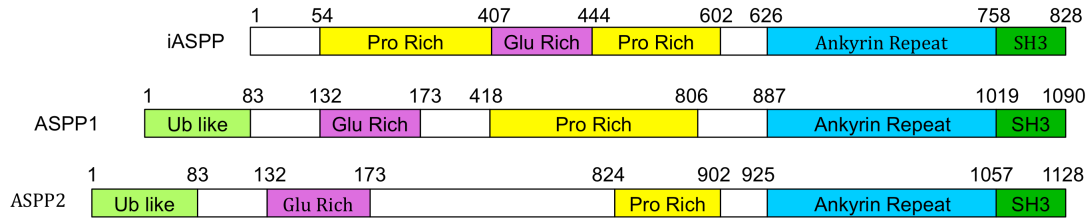


Figure 1. The domains of the ASPP protein family. The C-termini of the three family members contain ankyrin repeats and an SH3 domain. Likewise, they all share proline rich regions and glutamine rich regions. However, it is only ASPP1 and ASPP2 that possess a ubiquitin like domain. Ahn et al. 2009.



Figure 2. Structural similarity between ASPP family members. The structure of iASPP (PDB ID 2VGE) is depicted in blue and ASPP2 (PDB ID 1YCS) is shown in orange.

It is worth noting that the SH3 domain of ASPP2 contains the binding site for p53 which is slightly different than previously characterized SH3 domain/protein interactions. (Robinson et al. 2008; Ahn et al. 2009; Mayer 2001). In this case, it is not the proline rich region of p53 that binds to ASPP2 (Ahn et al. 2009). However, there are some prolines present in the region of the p53 core domain that binds to the SH3 domain of ASPP2 (Robinson et al. 2008; Gorina et al. 1997). Recently, the crystal structure of ASPP2 bound to p73 was reported which confirmed earlier NMR studies which indicated that ASPP2 binds the DNA binding domain of p73 (Ahn et al. 2009; Canning et al. 2012). The putative p53 binding site of iASPP is also composed of the SH3 domain of this ASPP family member, which has been shown to bind to the linker region of p53 rather than the proline rich region (Ahn et al. 2009). However, the linker region of p53 (residues 289-322) does contain four proline residues that are thought to be critical for binding to the SH3 domain of iASPP (Ahn et al. 2009). These interactions are very important because the binding of iASPP to the tumor suppressors p53 and p73 results in the anti-apoptotic function of iASPP in cancer cells which suggests that iASPP may serve as a promising cancer target (Bergamaschi et al. 2003; Gillotin 2009; Bell et al. 2008). Indeed, iASPP can inhibit the tumor suppressors p53 and p73 that often prevent the formation of tumors and stop cells with mutated or damaged DNA from propagating. Proteins, such as iASPP, that inhibit tumor suppressors can lead to cancer cell proliferation when they are over expressed (Bergamaschi et al. 2003; Robinson et al. 2008; Bell et al. 2008).



It has been shown that iASPP is over expressed in many cancer types, and silencing of this protein in cancer cell lines results in apoptosis or cell cycle arrest. Over expression of iASPP has been observed in leukemia, non-small cell lung cancer, ovarian cancer, glioblastoma, prostate, and liver cancers (Liu et al. 2009; Zhang et al. 2005; Jiang et al. 2011; Chen et al. 2012; Li et al. 2012; Li et al. 2011; Zhang et al. 2011; Lin et al. 2011; Deng et al. 2010). In non-small cell lung cancer, iASPP over expression is associated with both metastasis and a decreased response to chemotherapy (Chen et al. 2010; Su et al. 2007). Moreover, silencing of iASPP in leukemia, breast, glioblastoma, non-small cell lung cancer, ovarian, prostate, and liver cancer cell lines results in an increase in cell death (Chen et al. 2012; Li et al. 2011; Liu et al. 2009; Liu et al. 2008; Jiang et al. 2011; Lin et al. 2011). Taken together, these studies suggest that iASPP may be a promising target for therapeutic inhibition for many cancer types.

It is the role of iASPP in the p53 pathway (Figure 3) that makes iASPP so tantalizing as a target. In response to oncogenic stress such as DNA breaks or the presence of lesions in DNA, p53 activates genes coding for pro-apoptotic and cell cycle arrest proteins including, but not limited to, Bax, PUMA, p21, DR5, and Fas, (Menendez et al. 2009). The up-regulation of these proteins leads to cell death or cell cycle arrest in cells experiencing oncogenic stress (Menendez et al. 2009; Sullivan et al. 2007). There are also many co-factors that bind to p53 and promote the transactivation of specific p53 targets (Harms et al. 2004; Sullivan et al. 2007). ASPP1 and ASPP2 are among the cofactors that influence the ability of p53 to bind pro-apoptotic target genes (Bell et al. 2007; Bell et al. 2008). iASPP, however, blocks the ability of p53 to transactivate its pro-

apoptotic and pro-cell cycle arrest targets (Bell et al. 2007; Bergamaschi et al 2003; Robinson et al. 2008). Thus, the tumor suppressor function of p53 is inhibited by iASPP allowing cancer cells to abberantly proliferate (Bergamaschi et al 2003; Bell et al 2007; Bell et al. 2008). Removal of iASPP's inhibition of p53 may restore the apoptotic or cell cycle arrest function of p53, thereby, leading to a reduction in the number of cancer cells.

This hypothesis assumes that p53 is not mutated and is functional. However, p53 is mutated or deleted in half of all human tumors (Hollstein et al. 1991). In these cancers, iASPP could still function by binding to a related tumor suppressor protein, p73. p73, like p53, functions as a tumor suppressor by transactivating pro-apoptotic and cell cycle arrest genes in cells experiencing oncogenic stress (Bell et al. 2007). In fact, these two proteins share many of the same downstream pro-apoptotic and cell cycle arrest target genes (Bell et al. 2007).

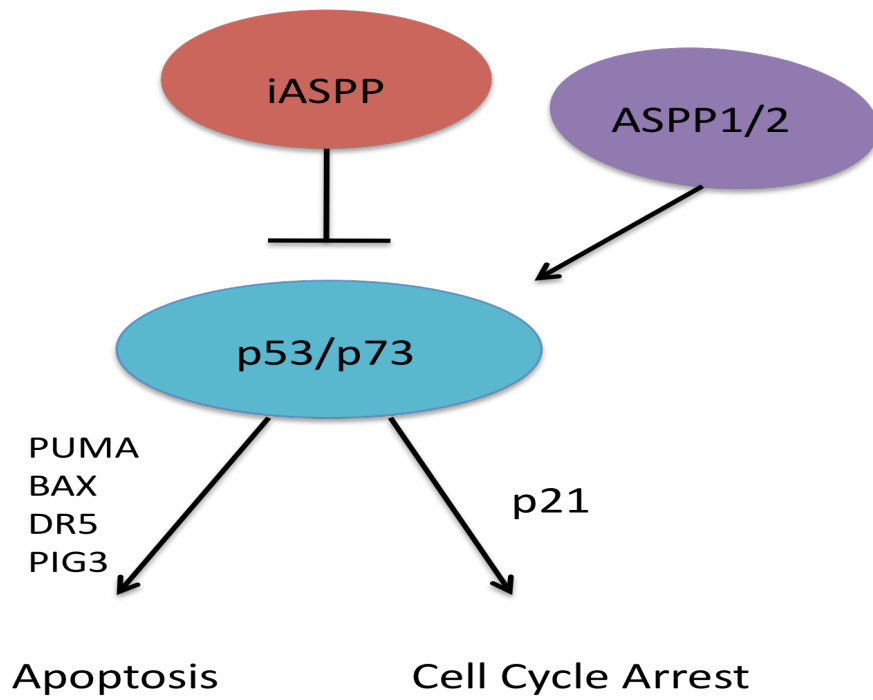


Figure 3. Abbreviated p53/p73 pathway. p53 transactivates many target genes resulting in cell cycle arrest or apoptosis. iASPP can inhibit both p53 and p73.

In support of this hypothesis, iASPP inhibition has been shown to lead to an increase in apoptosis via p73 (Bell et al. 2007). This data suggests that inhibiting iASPP may be a viable option as a cancer therapy in patients where iASPP is over expressed and p53 is non-functional. This is supported by data on iASPP inhibition generated by the Ryan Lab which demonstrated that disruption of the iASPP-p73 interaction by a 37 amino acid peptide resulted in a dramatic reduction in tumor size in a mouse xenograft model (Bell et al. 2007). This 37 amino acid peptide (37-mer) was shown to disrupt the interaction between iASPP and p73 in cell lines and *in vivo* models (Bell et al. 2007). By the disruption of this protein-protein interaction, the number of cancer cells was significantly reduced compared to non-transformed cells (Bell et al. 2007). These data were the same for cancer cells containing p53 as well as cancer cells lacking functional p53 (Bell et al. 2007). Additionally, the down stream targets of p53 and p73 were induced upon iASPP inhibition (Bell et al. 2007). These results further indicate that targeting iASPP may be an effective new strategy for treating many types of cancer, including cancers that lack functional p53.

In order to determine if iASPP is a viable protein to target in the search for new cancer therapies, we needed to establish the following: 1) whether iASPP is druggable with a small molecule inhibitor 2) whether robust and efficient assays can be developed to functionally evaluate small molecules that bind to iASPP, and 3) whether we can verify and further validate iASPP as a potential cancer target through the use of RNAi. For my thesis, I investigated the first two criteria, and while a fellow lab member, Bhavaratini Vangamudi, simultaneously investigated the third criterion.

To establish whether iASPP is a druggable protein target, we pursued a fragment-based approach where it has been shown that the hit rate obtained in a fragment-based screen is correlated to the druggability of the protein (Hajduk et al. 2007). Towards this end, iASPP was cloned, expressed, labeled, purified, and screened against our library of 15,000 chemical fragments by NMR. In this case, we used a SOFAST-HMQC experiment to screen for chemical fragments that bind to  $^{15}\text{N}$  labeled iASPP C-terminus (Schanda et al. 2005). Binding of fragments to iASPP causes measurable chemical shift changes of the amino acid residues perturbed by the binding. These chemical shift changes allow identification of fragments that bind to iASPP (“hits”) (Shuker et al. 1996). As a measure of druggability, a hit rate of 0.3% in a fragment-based screen results in the development of a small molecule inhibitor 80% of the time in the cases studied (Hajduk et al. 2007). In addition to being a useful indicator of protein druggability, these fragments serve as a starting point for the design of more potent inhibitors of iASPP (Hajduk et al. 2007; Shuker et al. 1996). Our goal was to compare the hit rate generated with iASPP to previously reported hit rates and obtain a measure of the druggability of iASPP; these data would guide us in determining whether or not we should pursue iASPP as a viable cancer target in our lab.

In order to meet our second criteria, we sought to develop an FPA (fluorescence polarization anisotropy) assay in order to measure the disruption of the interaction between iASPP and peptides that bind to iASPP (Souza-Fagundes et al. 2012). Successful development of an assay that is reliable, reproducible, and efficient to measure the ability of a small molecule to disrupt this interaction is critical.

## CHAPTER II

### PREPARATION OF iASPP FOR FRAGMENT-BASED SCREENING

#### Introduction

The first step toward conducting a fragment-based screen using NMR is to produce purified isotopically labeled protein in sufficient amounts to complete the screen. Preparation of the protein involves designing and testing different constructs, recombinant expression of our constructs for optimal protein expression levels, and optimizing the buffer conditions of the NMR sample to obtain the best NMR spectrum.

#### Methods

Each construct was expressed in electrocompetent *E. coli* strains BL21 Gold, BL21 RIL, Rosetta 2, and Rosetta 2 RIL for expression testing. The constructs were optimized for expression in M9 minimal media in small scale of 5 ml before optimizing expression of the protein in 1.5 liters of media in baffled flasks. For expression testing, a series of experiments were performed for each construct and each *E. coli* strain. For each, the protein was induced with IPTG (isopropyl  $\beta$ -D-1-thiogalactopyranoside) at 37°C for 5 hours, 25°C for 5 and 16-18 hours, or 18°C for 16-18 hours. The culture was then centrifuged at 3,000 x g for 15 minutes and the supernatant was discarded. The cell pellet was then re-suspended in phosphate buffer and sonicated at 4°C to lyse the cells. The cell lysate was then centrifuged, and the supernatant was collected for SDS-PAGE analysis of

protein expression. Protein expression was determined by the appearance of a band on the PAGE gel at the appropriate molecular weight where no band is present in the un-induced samples. For expression trials, the buffer contained 50 mM phosphate, 100 mM NaCl, and 5 mM DTT. Once expression was established, optimization of the purification of the protein was the next step. All constructs had a 6-His tag for nickel column chromatography. Unbound protein was washed from the nickel column with a minimum of four column volumes of buffer containing 20 mM imidazole before bound protein was eluted with a gradient of increasing imidazole concentrations from 20 mM to 500 mM imidazole. For constructs with a TEV (tobacco etch virus) protease cleavage site, TEV protease was added and subtractive nickel column chromatography was performed. For purification of the constructs without a TEV cleavage site, a size exclusion chromatography step was added. In some cases, we also conducted ion exchange chromatography to obtain a more pure sample that was free of aggregates and impurities.

Following the production of recombinantly expressed and purified iASPP, a two-dimensional  $^1\text{H}/^{15}\text{N}$  correlation spectrum was collected in those cases where a sufficient yield of the protein was obtained. We chose to perform a  $^1\text{H}/^{15}\text{N}$  SOFAST-HMQC spectrum because SOFAST-HMQC has an advantage of shorter inter scan delays allowing more repetitions of the experiment in shorter time which results in a the signal to noise increase compared to the HMQC experiment. (Schanda et al. 2005).

## Results

Initially, we selected the iASPP C-terminal construct  $\Delta 623-828$  because it contains the SH3 domain (the domain we wish to inhibit) and the ankyrin repeats. It is imperative to express the SH3 domain with the ankyrin repeats because the SH3 domain alone is not stable and does not express well. This particular construct was also reported by Ahn et al in their work. Thus, there is literature precedent for the recombinant expression of this construct. We cloned  $\Delta 623-828$  into an expression vector containing an N-terminus His-tag. We expressed this construct in four strains of electrocompetent *E. coli* (BL21 Gold, BL21 RIL, Rosetta 2, and Rosetta 2 RIL). The level of expression was low for each strain. We observed that protein expression levels were poor for protein expressed at 37°C for 5 hours or 25°C for 16-18 hours. This level of expression (estimated at less than 10 mg/L) was insufficient to generate enough protein to conduct the screen. However, when the protein was expressed at 18°C for 16-18 hours, sufficient protein was expressed to allow purification (40 mg/L).

After obtaining purified protein, we collected spectra of iASPP in order to determine if our construct would be suitable for screening by NMR. In order to determine if our construct was indeed suitable for conducting a fragment-based screen, which is conducted in mixtures of 12 fragments, we collected a SOFAST-HMQC spectrum of iASPP  $\Delta 623-608$  in the presence (Figure 4) and absence of a fragment mixture. The spectrum of iASPP in Figure 4 with the fragment mixture clearly shows the protein is precipitating. The spectrum of iASPP alone was similar to the published spectrum of iASPP (Ahn et al. 2009). Furthermore, this construct was not stable at room temperature



for more than a few hours. For the screen, we must have protein that can withstand room temperature conditions for several hours in order to facilitate the efficient screening of our fragment library, and the protein must be stable when combined with our fragment mixtures. To test whether our purified protein was free from all aggregates, we extended our purification scheme to include size exclusion and anion exchange columns. In addition, we tried to reduce the concentration of our fragment mixture in half (400  $\mu$ M vs 800  $\mu$ M). Unfortunately, we were unable to see any improvement in the quality of our NMR spectra.

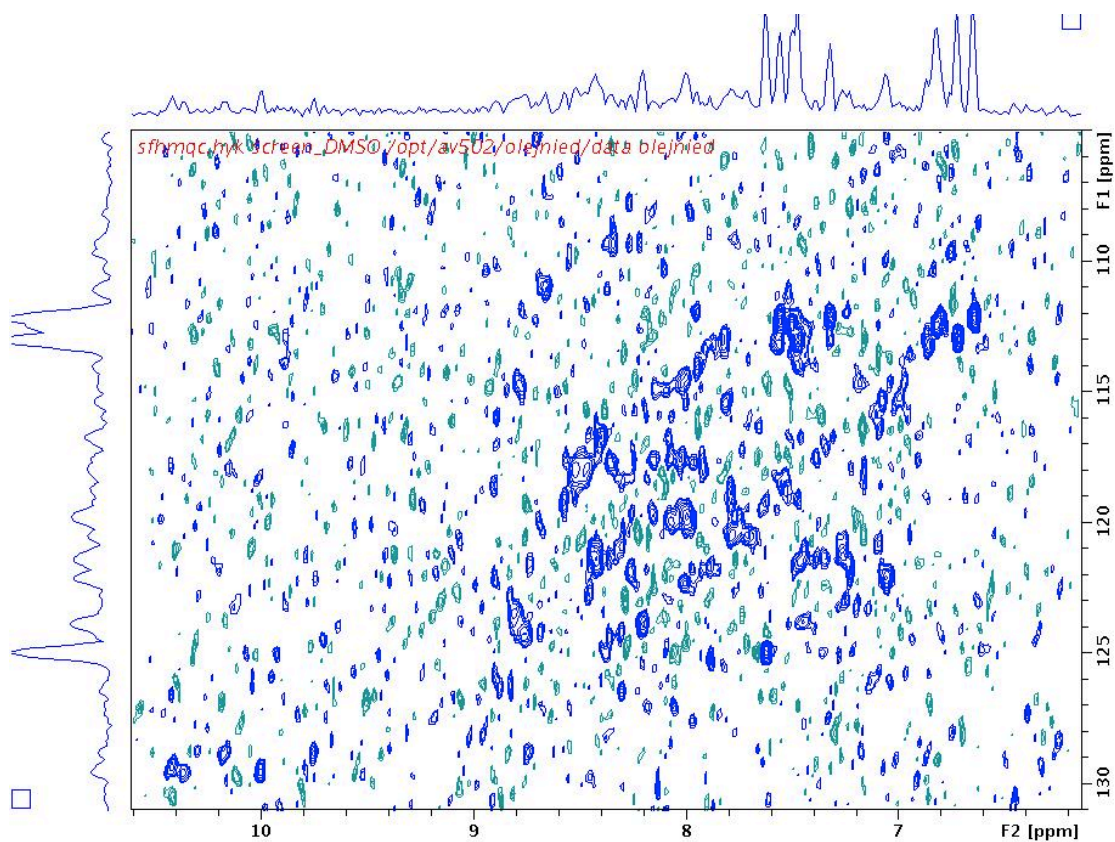


Figure 4. SOFAST-HMQC spectrum of  $\Delta 623-828$  iASPP with a fragment mixture. This spectrum demonstrates the poor quality of spectra that result from this construct of iASPP when fragments are present.

In order to conduct the fragment screen, it was imperative to improve the stability of the protein. We experimented with varying salt conditions and buffers in an attempt to increase the stability. Initially, we maintained a 50 mM phosphate buffer with 5 mM DTT while varying the type and concentrations of salt. At a pH of 7.3, we tested our protein with 50 mM NaCl, 100 mM NaCl, 150 mM NaCl, 200 mM NaCl in 50 mM phosphate and 5 mM DTT. None of these NaCl concentrations improved the stability of the protein. In fact, at 50 mM NaCl, the protein visibly precipitated in the presence of the fragment mixture. We also tried KCl and MgCl<sub>2</sub> with and without NaCl. NaCl was maintained at 100 mM to balance the stabilizing effect of the salt while varying the concentrations of KCl and MgCl<sub>2</sub>. We tested many salt and buffer conditions including:

- 1) 50 mM KCl, 100 mM NaCl, 50 mM PO<sub>4</sub>, 5 mM DTT
- 2) 100 mM KCl, 100 mM NaCl, 50 mM PO<sub>4</sub>, 5 mM DTT
- 3) 150 mM KCl, 100 mM NaCl, 50 mM PO<sub>4</sub>, 5 mM DTT
- 4) 200 mM KCl, 100 mM NaCl, 50 mM PO<sub>4</sub>, 5 mM DTT
- 5) 100 mM KCl, 50 mM PO<sub>4</sub>, 5 mM DTT
- 6) 150 mM KCl, 50 mM PO<sub>4</sub>, 5 mM DTT
- 7) 200 mM KCl, 50 mM PO<sub>4</sub>, 5 mM DTT
- 8) 50 mM MgCl<sub>2</sub>, 100 mM NaCl, 50 mM PO<sub>4</sub>, 5 mM DTT
- 9) 50 mM MgCl<sub>2</sub>, 150 mM NaCl, 50 mM PO<sub>4</sub>, 5 mM DTT
- 10) 150 mM MgCl<sub>2</sub>, 100 mM NaCl, 50 mM PO<sub>4</sub>, 5 mM DTT
- 11) 50 mM MgCl<sub>2</sub>, 50 mM PO<sub>4</sub>, 5 mM DTT
- 12) 100 mM MgCl<sub>2</sub>, 50 mM PO<sub>4</sub>, 5 mM DTT
- 13) 150 mM MgCl<sub>2</sub>, 50 mM PO<sub>4</sub>, 5 mM DTT
- 14) 200 mM MgCl<sub>2</sub>, 50 mM PO<sub>4</sub>, 5 mM DTT
- 15) 50 mM KCl, 50 mM MgCl<sub>2</sub>, 50 mM NaCl, 50 mM PO<sub>4</sub>, 5 mM DTT
- 16) 50 mM KCl, 50 mM MgCl<sub>2</sub>, 50 mM PO<sub>4</sub>, 5 mM DTT
- 17) 50 mM KCl, 50 mM MgCl<sub>2</sub>, 50 mM PO<sub>4</sub>, 5 mM DTT
- 18) 50 mM KCl, 100 mM MgCl<sub>2</sub>, 50 mM PO<sub>4</sub>, 5 mM DTT
- 19) 50 mM KCl, 150 mM MgCl<sub>2</sub>, 50 mM PO<sub>4</sub>, 5 mM DTT
- 20) 100 mM NaCl, 50 mM PO<sub>4</sub>, 5 mM DTT

mM PO<sub>4</sub>, 5 mM DTT. None of these conditions offered any improvement in the quality of the NMR spectrum of the protein.

Next, we tried adding ammonium sulfate, which is known to have a stabilizing effect on proteins. However, this salt can also precipitate or “salt out” a protein very quickly; thus, we used a total concentration of 25 mM in order to avoid salting out our protein while enhancing its stability. We tried the following: 1) 50 mM PO<sub>4</sub>, 100 mM NaCl, 25 mM NH<sub>2</sub>SO<sub>4</sub>, 5 mM DTT 2) 50 mM PO<sub>4</sub>, 150 mM NaCl, 25 mM NH<sub>2</sub>SO<sub>4</sub>, 5 mM DTT 3) 50 mM PO<sub>4</sub>, 100 mM KCl, 25 mM NH<sub>2</sub>SO<sub>4</sub>, 5 mM DTT 4) 50 mM PO<sub>4</sub>, 100 mM NaCl, 100 mM MgCl<sub>2</sub>, 25 mM NH<sub>2</sub>SO<sub>4</sub>, 5 mM DTT 5) 50 mM PO<sub>4</sub>, 150 mM KCl, 25 mM NH<sub>2</sub>SO<sub>4</sub>, 5 mM DTT 6) 50 mM PO<sub>4</sub>, 100 mM KCl, 100 mM MgCl<sub>2</sub>, 25 mM NH<sub>2</sub>SO<sub>4</sub>, 5 mM DTT. Once again, we were unable to note any improvement in protein stability.

We also tried additional buffers, including HEPES (4-(2-hydroxyethyl)-1-piperazineethanesulfonic acid), Tris-HCl (Tris(hydroxymethyl)aminomethane hydrochloride), and MES (2-(N-morpholino) ethanesulfonic acid). The buffer conditions tested include: 1) 50 mM Tris-HCl, 100 mM NaCl, 25 mM NH<sub>2</sub>SO<sub>4</sub>, 5 mM DTT 2) 50 mM Tris-HCl, 100 mM NaCl, 5 mM DTT 3) 50 mM Tris-HCl, 100 mM NaCl, 100 mM MgCl<sub>2</sub>, 5 mM DTT 4) 50 mM Tris-HCl, 100 mM KCl, 100 mM MgCl<sub>2</sub>, 5 mM DTT 5) 50 mM Tris-HCl, 50 mM NaCl, 25 mM NH<sub>2</sub>SO<sub>4</sub>, 5 mM DTT 6) 50 mM HEPES, 100 mM NaCl, 25 mM NH<sub>2</sub>SO<sub>4</sub>, 5 mM DTT 7) 50 mM HEPES, 100 mM NaCl, 5 mM DTT 8) 50 mM HEPES, 100 mM NaCl, 100 mM MgCl<sub>2</sub>, 5 mM DTT 9) 50 mM HEPES, 100 mM KCl, 100 mM MgCl<sub>2</sub>, 5 mM DTT 10) 50 mM HEPES, 50 mM NaCl, 25 mM

NH<sub>2</sub>SO<sub>4</sub>, 5 mM DTT 11) 50 mM MES, 100 mM NaCl, 25 mM NH<sub>2</sub>SO<sub>4</sub>, 5 mM DTT 12) 50 mM MES, 100 mM NaCl, 5 mM DTT 13) 50 mM MES, 100 mM NaCl, 100 mM MgCl<sub>2</sub>, 5 mM DTT 14) 50 mM MES, 100 mM KCl, 100 mM MgCl<sub>2</sub>, 5 mM DTT 15) 50 mM MES, 50 mM NaCl, 25 mM NH<sub>2</sub>SO<sub>4</sub>, 5 mM DTT. None of these buffer conditions made any improvement in the stability of our protein.

The next logical parameter to optimize was the pH of the buffer solution. The theoretical isoelectric point of iASPP C-terminus is 4.4. We, therefore, chose to experiment with pH in the range of 6.0-8.0 in order to balance the need for less basic pH in our NMR experiments with the low pI of the protein. We chose the following buffer conditions in which to vary the pH. They are as follows: 1) 50 mM PO<sub>4</sub>, 100 mM NaCl, 25 mM NH<sub>2</sub>SO<sub>4</sub>, 5 mM DTT 2) 50 mM PO<sub>4</sub>, 100 mM NaCl, 5 mM DTT 3) 50 mM Tris-HCl, 100 mM NaCl, 5 mM DTT 4) 50 mM MgCl<sub>2</sub>, 100 mM NaCl, 50 mM PO<sub>4</sub>, 5 mM DTT 5) 50 mM MgCl<sub>2</sub>, 100 mM NaCl, 50 mM Tris-HCl, 5 mM DTT. For each of the conditions listed above, we then varied the pH. We tested the stability of the protein at pH 6.5, 7.0, 7.3, 7.5, 7.7, and 8.0. Creating a more acidic buffer condition of 6.5 worsened the apparent stability of the protein; no improvement or difference was observed in the spectrum compared to those collected at pH 7.3- 8.0.

Another possible reason for the poor quality NMR spectrum may have been our choice of reducing agent. While DTT is a common and effective reducing agent, it is more volatile than TCEP (tris(2-carboxyethyl)phosphine). Thus, we chose to experiment with TCEP as a reducing agent in our buffer system. However, TCEP is not very stable in phosphate

buffers near pH 7; therefore, we tested TCEP in Tris-HCl buffers in the following conditions: 1) 50 mM MgCl<sub>2</sub>, 100 mM NaCl, 50 mM Tris-HCl, 1 mM TCEP 2) 100 mM NaCl, 50 mM Tris-HCl, 1 mM TCEP 3) 50 mM Tris-HCl, 100 mM NaCl, 25 mM NH<sub>2</sub>SO<sub>4</sub>, 1 mM TCEP. Although no improvement in the spectrum was observed, we continued to use TCEP as our reducing agent because of its potency and because it is more stable over time in open solutions which would be more ideal for screening conditions.

Finally, we tested additives in order to improve the stability of our protein. The following conditions were tested: 1) 100 mM NaCl, 50 mM Tris-HCl, 1 mM TCEP, Ph 7.3 2) 50 mM Tris-HCl, 100 mM NaCl, 25 mM NH<sub>2</sub>SO<sub>4</sub>, 1 mM TCEP, pH 7.3 3) 50 mM MgCl<sub>2</sub>, 100 mM NaCl, 50 mM Tris-HCl, 1 mM TCEP, pH 7.3. Into each of these buffers, we added 1% glycerol, 2% glycerol, or 5% glycerol. Once again, we were unable to improve upon the stability of our protein. Because the C-terminus of iASPP does contain free cysteines, we chose to test whether the addition of iodoacetic acid might improve the stability, but no improvement was obtained.

Since all of our attempts to improve the stability of the protein and quality of the NMR spectra by altering the buffer conditions was not successful, we decided to test different constructs. For example, MBP (maltose binding protein) was added to the His-tag on the N-terminus of our construct. MBP is a popular chaperone protein capable of enhancing the folding and solubility of proteins during expression. We reasoned that our protein might benefit from such a chaperone protein. The buffer conditions used to test our new

construct included: 1) 100 mM NaCl, 50 mM Tris-HCl, 1 mM TCEP, pH 7.3 2) 50 mM Tris-HCl, 100 mM NaCl, 25 mM NH<sub>2</sub>SO<sub>4</sub>, 1 mM TCEP, pH 7.3 3) 50 mM MgCl<sub>2</sub>, 100 mM NaCl, 50 mM Tris-HCl, 1 mM TCEP, pH 7.3. No improvement was observed.

Therefore, we moved the His-tag to the C-terminus of our construct and tested the protein using the same three buffer conditions listed above. Once again, we saw no improvement in the ability of our protein to remain soluble or stable in our fragment mixtures.

Therefore, we abandoned our  $\Delta$ 623-828 construct altogether and selected four additional constructs for testing. In the first new construct, we mutated the free cysteines and created a C699S, C703S mutated form of  $\Delta$ 623-828. The second new construct ( $\Delta$ 608-828) was chosen because it was used to determine the crystal structure of iASPP (Robinson et al). The third new construct ( $\Delta$ 625-828) was chosen due to a report in the literature on the successful expression of iASPP (Robinson et al) The fourth construct, ( $\Delta$ 618-828) was chosen based on a secondary structure prediction of the C-terminus of iASPP in which a helix exists C-terminal to the first ankyrin repeat. This slightly longer construct (+5 residues) was selected to ensure that we were not truncating the protein in the middle of a helix. Despite many attempts to optimize the expression of constructs iASPP C699S and C703S,  $\Delta$ 623-828, iASPP  $\Delta$ 618-828, and iASPP  $\Delta$ 625-828 using many conditions, we were only able to express very small amounts of protein. In contrast, iASPP  $\Delta$ 608-828 overexpressed at 18°C overnight and was stable in 100 mM NaCl, 50 mM Tris-HCl, 1 mM TCEP, pH 7.3. Therefore, we tested the stability of the protein upon the addition of a fragment mixture and were pleased with the quality of the NMR spectrum (Figure 5). In order to verify that this protein binds to relevant binding

partners, we collected spectra of iASPP $\Delta$ 608-828 in the presence and absence of the two peptides: a p53 linker region and GSPRKARRA. (Figure 6 and Figure 7). iASPP C-terminus has been shown to bind to the p53 linker region and to GSPRKARRA (an iASPP derived peptide) (Ahn et al. 2009, Robinson et al. 2007). The chemical shift changes observed suggest that iASPP  $\Delta$ 608-828 may be a functional protein. Moreover, based on the expression levels obtained, and the stability of the protein in the absence and presence of fragment mixtures, we concluded that we had finally obtained a suitable construct and experimental conditions to conduct our fragment-based screening of iASPP by NMR.



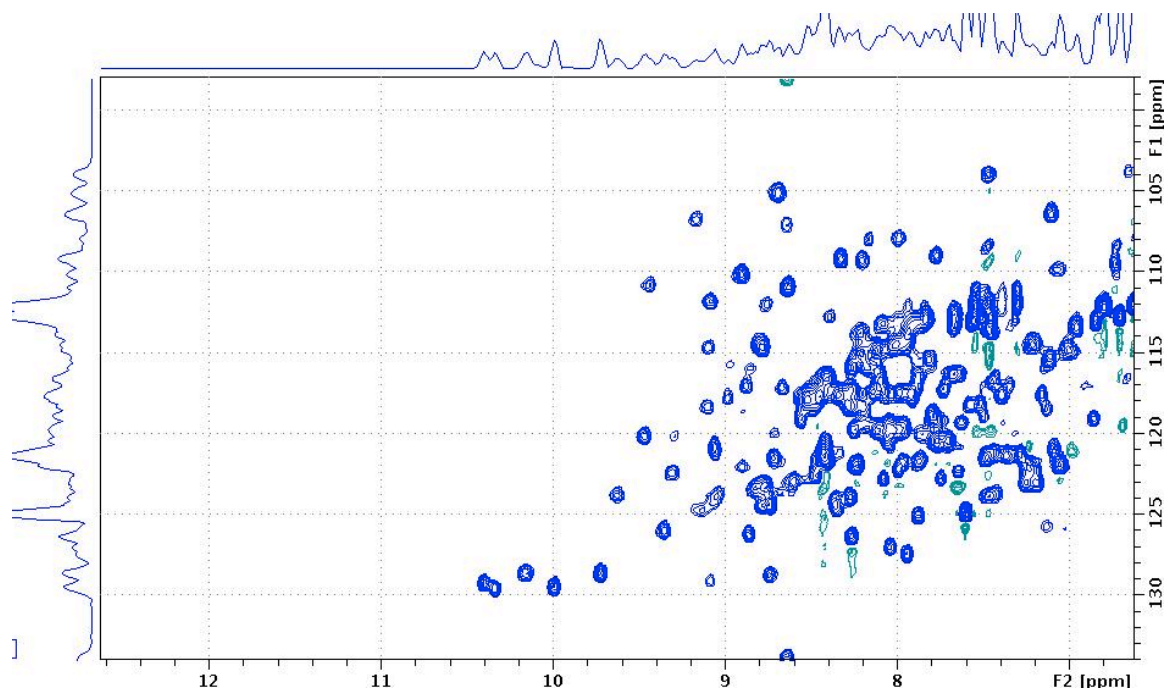


Figure 5. SOFAST-HMQC of iASPP  $\Delta$ 608-825 iASPP collected at 293K on 500 MHz NMR spectrometer with fragment mixture. This condition is stable for screening.

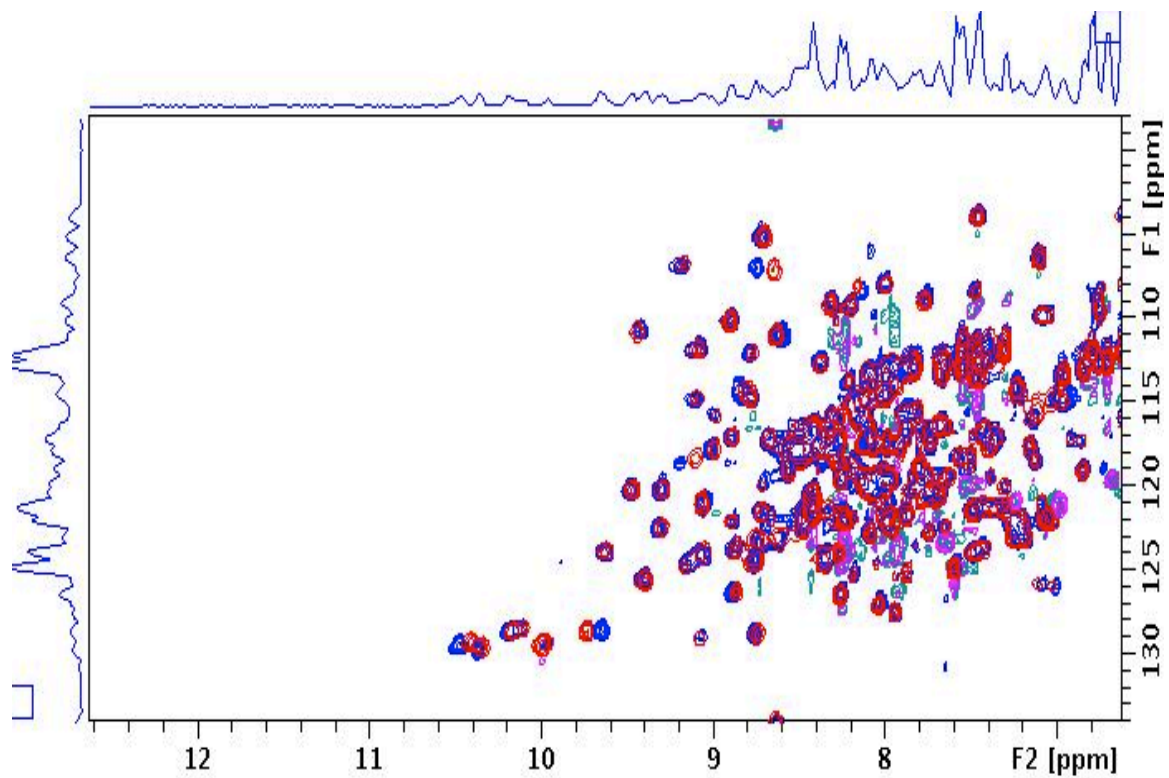


Figure 6. SOFAST-HMQC spectra of iASPP  $\Delta$ 608-828 bound to GSPRKARRA (blue) and free iASPP  $\Delta$ 608-828 (red). SOFAST-HMQC collected at 293K on 500 MHz NMR spectrometer.

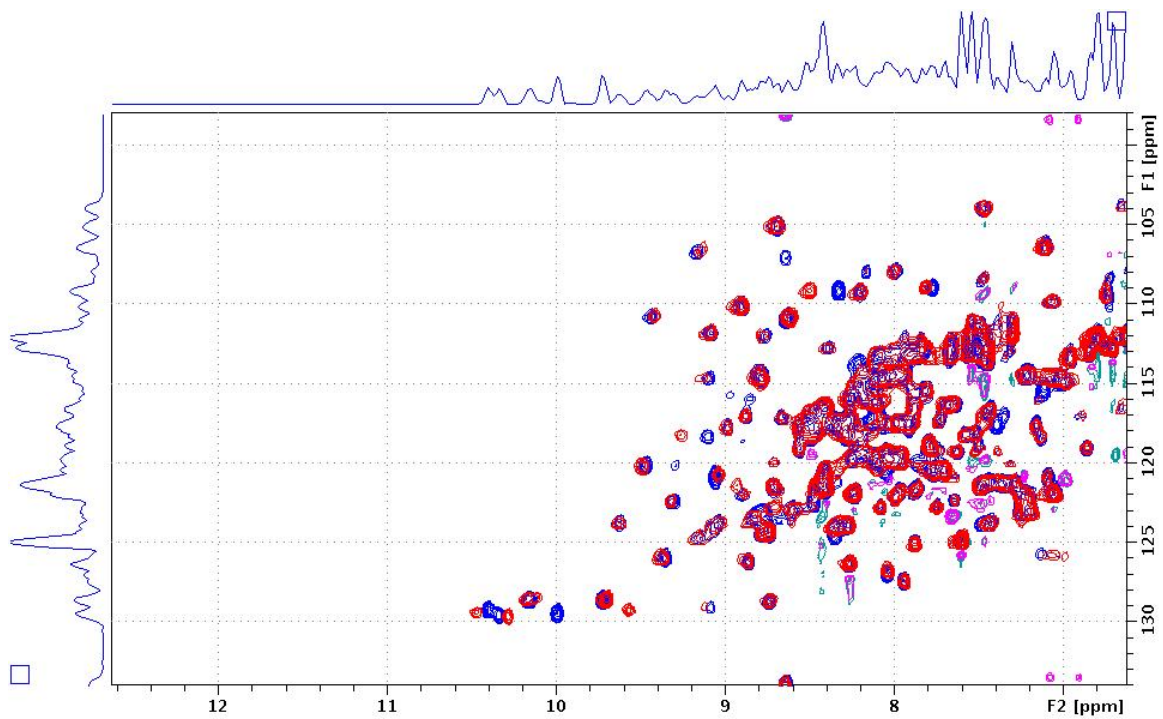


Figure 7. iASPP  $\Delta 608-828$  bound to p53 linker region (blue) and free iASPP  $\Delta 608-828$  (red). SOFAST-HMQC collected at 293K on 500 MHz NMR spectrometer.

## CHAPER III

### FRAGMENT-BASED SCREEN

#### Introduction

In order to determine whether iASPP is a druggable target, we conducted a fragment-based screen using NMR. This has been shown to be a useful approach to determine whether a particular protein is druggable. Based on an earlier publication by Hajduk et al., a protein is likely druggable if the percentage of fragments that bind to the protein target is greater than 0.3% (Hajduk et al. 2007). In that study, 58 protein targets that were the subject of fragment-based drug design efforts were used. For protein targets where the hit rate was less than 0.1%, potent small molecule inhibitors were developed in only 3.2% of cases. For protein targets with a hit rate of 0.1-0.3%, a potent small molecule inhibitor was developed in 31% of these cases, and, encouragingly, for hit rates exceeding 0.3%, potent small molecule inhibitors were developed in 82% of the targets studied (Hajduk et al. 2007). In addition to being a valuable tool to investigate whether a protein target is druggable, fragment-based screens are a proven method for identifying fragments that can become the initial chemical matter needed to develop potent small molecule inhibitors.

## Experimental Design

iASPP residues 608-828 were recombinantly expressed and uniformly isotopically labeled with  $^{15}\text{N}$  as described in chapter 2. Once sufficient quantities were obtained, iASPP was screened against our fragment library containing 15,000 compounds. Figure 8 outlines the experimental approach for conducting the screen. To reduce the number of NMR spectra that we needed to collect as well as the amount of protein required to complete the screen, we screened the fragment library in mixtures containing 12 compounds. Chemical shift changes observed upon the addition of compound mixtures, indicated that one or more compounds in the mixture was binding to iASPP. A score of 1-5, based on the magnitude of the observed chemical shift changes, was assigned to each mixture. A score of 5 indicates a chemical shift change of about 0.5 ppm or greater; whereas, a score of 3 indicates a chemical shift change of about 0.25 ppm. Mixtures with a score of 3 or higher were selected for de-convolution of the mixture in order to determine which fragment(s) was binding to iASPP. It is important to note that our scoring system does not imply a direct correlation with binding affinity because some compounds can induce a larger chemical shift change with lower affinity (e.g. compounds containing an aromatic ring). Once individual fragments have been identified, titrations were performed in order to determine their binding affinity. Once this is complete, we selected analogs of the fragments identified and screened these individually.

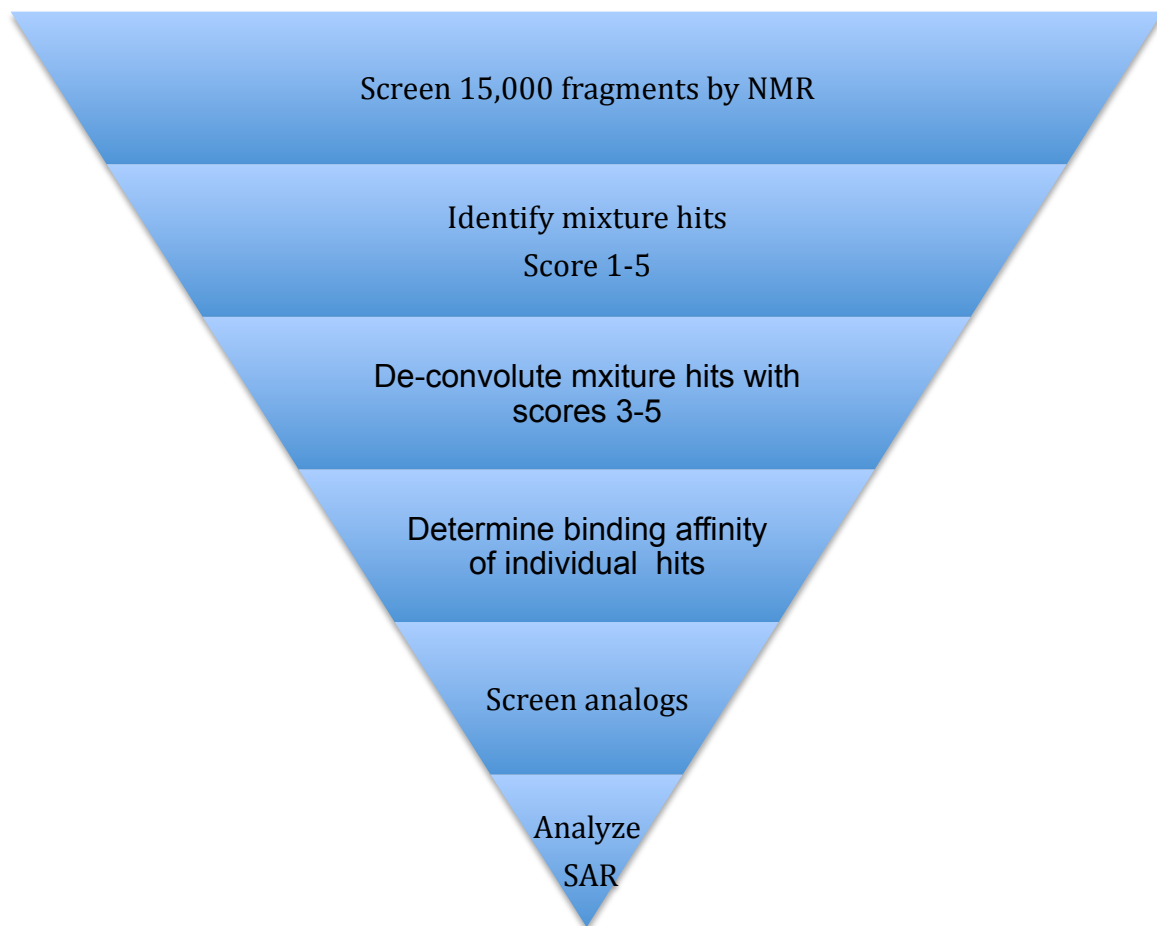


Figure 8. NMR fragment-based screen to identify fragments that bind to iASPP

In choosing how best to screen iASPP against our fragment library by NMR, we had to select which experiment would give us the most information in the most efficient way possible. We considered both HSQC (heteronuclear single quantum coherence) and SOFAST-HMQC (selective optimized flip angle short transient - heteronuclear multiple quantum coherence) experiments. TROSY-HSQC (transverse relaxation optimized spectroscopy - heteronuclear single quantum coherence) spectra of deuterated iASPP collected on a 900 MHz magnet have been previously reported by Ahn et al. However, for conducting this type of screen, we must obtain the best possible spectra on a 500 MHz or 600 MHz magnet because these NMR spectrometers have a sample changer and we did not want to incur the expense of deuterating the protein. SOFAST-HMQC has the advantage of allowing shorter inter scan delays and more repetitions of the experiment in a shorter time, using this experiment, the signal to noise is increased compared to HMQC. Before we were able to begin our screen, we optimized the protein concentration and optimized the parameters of the SOFAST-HMQC experiment to obtain the best signal to noise possible.

### Method

iASPP was recombinantly expressed and isotopically labeled as described in chapter 2. In order to determine the concentration of iASPP to be used in our NMR experiments, we collected spectra at 40  $\mu$ M, 50  $\mu$ M, 75  $\mu$ M, 100  $\mu$ M, 150  $\mu$ M iASPP. As expected, 150  $\mu$ M iASPP resulted in a stronger signal. However, we discovered that 50  $\mu$ M iASPP resulted in a sufficient signal and spectra for screening purposes. This finding is an advantage given that the screen requires a large amount of protein to complete, and each

batch of protein must be prepared freshly as iASPP becomes unstable during the freeze-thaw process. For the fragment-based screen, iASPP was concentrated to a final concentration of 50  $\mu\text{M}$  in 50 mM Tris-HCl, 100 mM NaCl, 1 mM TCEP, and 5 % deuterated DMSO. Fragment mixtures of 12 were added to each sample of iASPP with a final concentration of either 400  $\mu\text{M}$  or 800  $\mu\text{M}$  for each fragment. SOFAST-HMQC NMR experiments were conducted on a Bruker 500 MHz or 600 MHz NMR spectrometer at 293K. Spectral analysis was conducted using TopSpin software. Spectra from the fragment mixtures were overlaid with a spectrum of free iASPP. For any spectrum in which we observed chemical shift perturbations relative to the reference spectrum, we identified a fragment hit. We then de-convolved the 12 individual fragments for the mixtures that contained these fragment hits. By de-convolving the mixtures, we are able to identify those individual fragments that bind to iASPP. We then determined the binding affinities of the fragments by performing NMR titration experiments. For each titration experiment, the fragment was added to 50  $\mu\text{M}$  iASPP at final concentrations of 800  $\mu\text{M}$ , 600  $\mu\text{M}$ , 400  $\mu\text{M}$ , 200  $\mu\text{M}$ , 100  $\mu\text{M}$ , 50  $\mu\text{M}$  and 25  $\mu\text{M}$ . The magnitude of the change in chemical shift was measured and plotted against the concentration of fragment. From this plot, we extrapolated the binding affinity ( $K_d$ ) of the fragment.



## Results

The spectra in Figure 9 illustrate an example of the  $^1\text{H}/^{15}\text{N}$  chemical shift changes observed upon the addition of one of our fragment hits. Upon binding to the p53 linker region, iASPP exhibits chemical shift changes at W798 and W800. For most of our fragment hits, we also observe a chemical shift perturbation at W798 and/or W800.

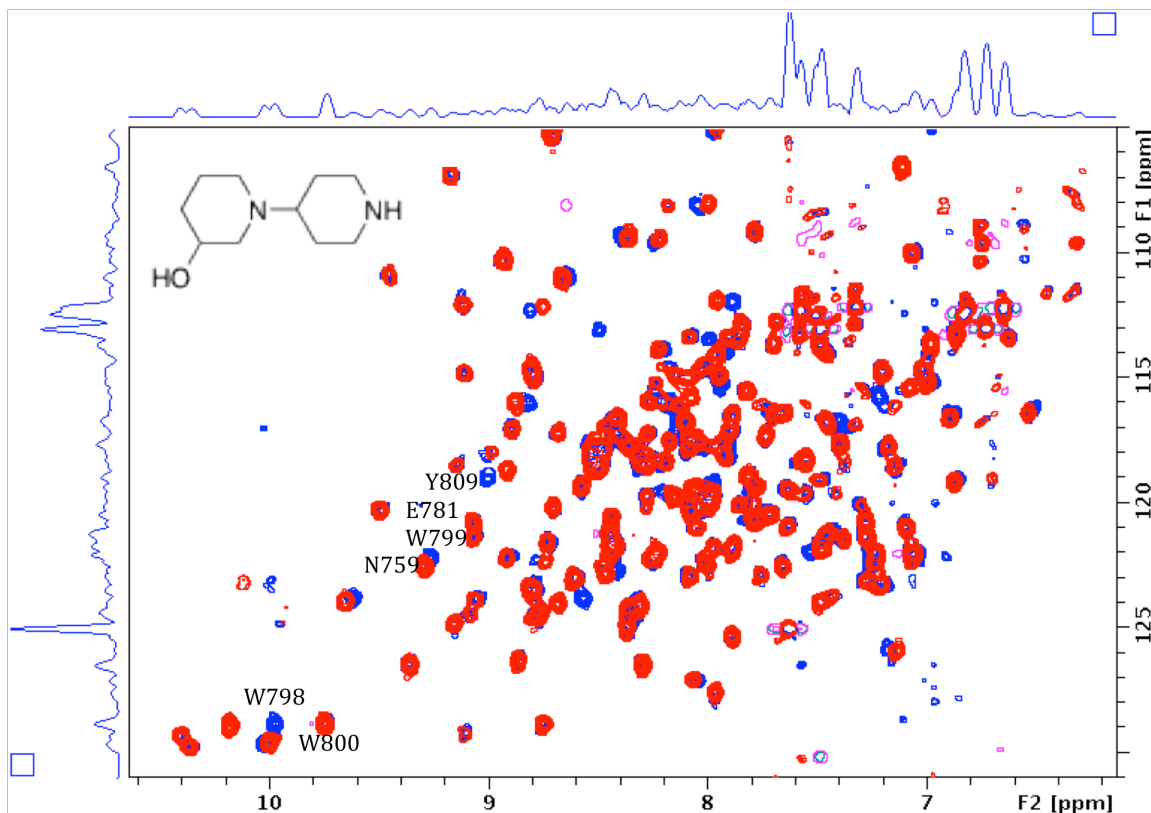
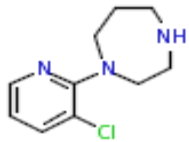
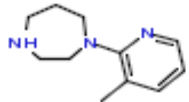
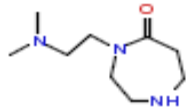
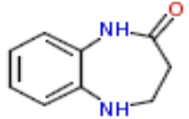
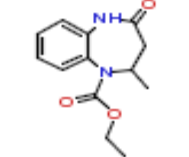


Figure 9. A fragment identified as binding to iASPP. A chemical shift perturbation is observed at W798, one of the W residues that experiences a chemical shift change when p53 binds to iASPP. SOFAST-HMQC, 600 MHz, 293K, 50  $\mu\text{M}$  iASPP. The assignments shown in this figure were reported by Ahn et al.

From our fragment mixtures, we identified two mixtures with a score of 5, indicating a rather large difference in the chemical shifts of unbound iASPP and iASPP bound to fragments. We discovered five mixtures with scores of 4 and thirty-seven mixtures with scores of 3. There were 71 mixtures with a score of 2 and 198 mixtures with a score of 1. We chose to de-convolute mixtures with scores of 3 or greater. Our hit rate from scores of 2 or greater is 0.8%. This indicates that iASPP is likely to be a druggable protein target.

We characterized the fragments by their chemical class and begin to discern some of the structure activity relationships of these fragments. The diazapane class is outlined in Table 1. It is interesting to note that the addition of a chlorine to the pyridyl group increases the affinity of the fragment to iASPP by an order of magnitude compared to the pyridyl-diazapane with a methyl side group. Following the discovery of the diazapanes, we measured the binding of azapane compounds which are similar in structure; none of our azapane compounds bound to iASPP. Substitution of the pyridyl group for either a benzyl or ethylamine group and a oxygen at the 2 position on the diazapane ring either further reduces the affinity of the fragment for iASPP or renders the compound unable to bind to iASPP.

Table 1. Diazapane fragments and approximate binding affinities

	$K_d = 309 \mu\text{M}$
	$K_d = 2.64 \text{ mM}$
	$K_d = 3.55 \text{ mM}$
	No binding
	No binding

Another class of compounds that we discovered bind to iASPP is the quinoline series shown in Table 2 and Table 3. For 2-ring compounds in the quinoline series possessing an amine group at the carbon 2 position and methyl groups at the carbon 5 and 7 position, adding a methyl at carbon 6 gives a slight increase in affinity. However, placing a fluoro- at carbon 6 and either a hydroxyl or amine group at carbon 4 diminishes the binding affinity for quinolines to iASPP. Table 3 is a continuation of our investigation of the quinoline series of fragments that further illuminates which fragments might be best suited as the starting material for any potential small molecule inhibitor of iASPP.

Table 2. Quinoline fragments with 2-ring structure approximate  $K_d$  values.

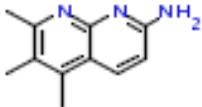
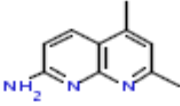
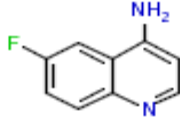
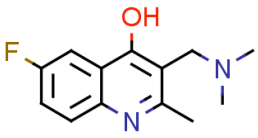
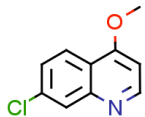
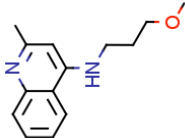
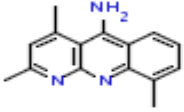
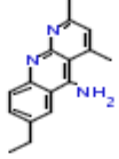
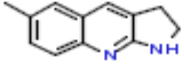
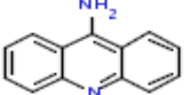
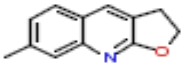
	$K_d = 650 \mu\text{M}$
	$K_d = 570 \mu\text{M}$
	$K_d = 1.64 \text{ mM}$
	$K_d = 2.27 \text{ mM}$
	No binding
	No binding

Table 3 outlines the results from our continued study of the quinoline series as we expand into quinolines with a 3-ring structure. Adding a benzyl to the quinoline structure where two methyl groups and an amino side group are already present, significantly increases the affinity of these fragments to iASPP. Removing the ethyl and methyl groups from this structure results in a large decrease in affinity. Removal of all but the amine side group also drastically decreases affinity. The addition of a pyrrolidone or furan in place of the benzyl group on the quinoline structure decreases or completely obliterates the ability of the fragment to bind to iASPP. This insight reveals that some members of the quinoline series are good candidates for becoming initial chemical matter in a small molecule inhibitor while the negative data in the series indicates where the specificity lies in these fragments.

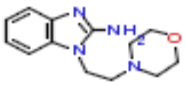
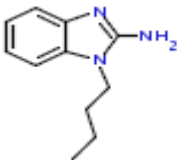
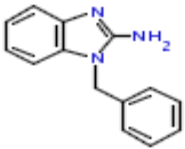
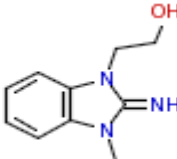
Table 3. Quinoline fragments with a 3-ring structure and approximate  $K_d$  values.

	$K_d = 110 \mu\text{M}$
	$K_d = 370 \mu\text{M}$
	$K_d = 1.89 \text{ mM}$
	$K_d = 1.59 \text{ mM}$
	No binding

A third series, amino-benzimidazole series, was also discovered. Table 4 is a summary of these fragments that we investigated as potential ligands to iASPP. Two of these fragments are observed as having micromolar binding affinities and may be suitable to

develop further into a small molecule inhibitor. It is clear, however, that adding benzyl or hydroxyl groups decreases the affinity four or five fold.

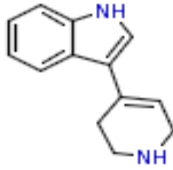
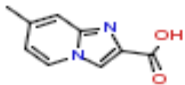
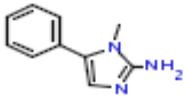
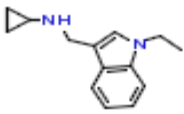
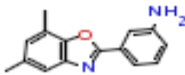
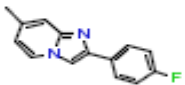
Table 4. Amino-benzimidazole series and approximate binding affinities.

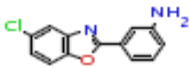
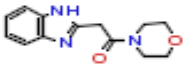
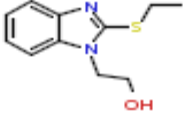
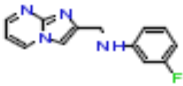
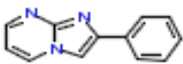
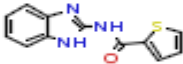
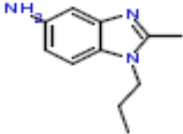
	$K_d = 420 \mu\text{M}$
	$K_d = 660 \mu\text{M}$
	$K_d = 2.05 \text{ mM}$
	$K_d = 2.80 \text{ mM}$

Once we had obtained the data for the amino-benzo-imidazole class of compounds listed above, we then obtained compounds with similar structures as shown in Table 5.



Table 5. Compounds with similar structure to the amino-benzoimidazole compounds

	$K_d = 3.77 \text{ mM}$
	$K_d = 554 \text{ }\mu\text{M}$
	$K_d = 827 \text{ }\mu\text{M}$
	$K_d = 1.27 \text{ mM}$
	No binding
	No binding

	No binding
	No binding
	No binding
	No Binding
	No binding
	No binding
	No binding

When the amine group at the 2 position is replaced with a thiol group, affinity is completely lost compared to the same 2-amino-benzimidazole with a hydroxyl ethyl group at the 1 position. We also see that when an amine is added to the benzene ring of the benzimidazole and the amine at the 2 position is replaced with a methyl group that affinity is lost completely. In general, the addition of fluorine and sulfur groups results in a complete loss of binding. While incorporating oxygen into the ring structure also results in a complete loss of binding. However, we are able to narrow this class of compounds down to a few that are below 1 mM in affinity and have the potential to become the initial chemical matter from which a small molecule inhibitor could be designed.

In order to complete this work, over 1,500 NMR experiments were performed and analyzed. We identified a hit rate for iASPP of approximately 0.9% indicating that it is likely possible to build a small molecule inhibitor to iASPP from the initial chemical matter identified in a second site screen. Thus, we are able to conclude that iASPP is a druggable target. We were also able to establish a few types of fragments that share similar chemical structures and were able to determine, to a degree, which components of these fragments are important for binding and increasing affinity to iASPP. Thus, we have also established a number of fragments with the potential to be further developed into a small molecule inhibitor of iASPP.

## CHAPTER IV

### ASSAY DEVELOPMENT

#### Introduction

For drug discovery, it is imperative that robust assays can be developed in order to follow the SAR (structure activity relationship) of any chemical compounds that inhibit the target protein. These assays are critical to any program designed to investigate a drug target and to all drug discovery programs. Thus, as part of my studies, I attempted to develop assays to characterize the compounds that bind to iASPP. These involve assays that measure the ability of compounds to disrupt iASPP from binding to peptides in the putative p53 binding site using a FPA (fluorescence polarization anisotropy) assay.

#### Experimental Design

We pursued the development of an FPA assay to evaluate small molecule inhibitors of iASPP. The principle of this assay (Figure 10) is that we are able to distinguish between labeled peptides bound to iASPP and labeled peptides that are unbound in solution with iASPP. Using this method, anisotropy increases as the binding of fluorophore labeled peptide to protein increases. The polarized light is measured, and anisotropy ( $r$ ) can then be calculated by the formula:  $r = \frac{I_{\parallel} - I_{\perp}}{I_{\parallel} + 2I_{\perp}}$  (Rossi et al. 2011; Souza-Fagundes et al. 2012).  $I_{\parallel}$  equals the intensity of light detected that is parallel to the plane of polarization of light used to excite the fluorophore.  $I_{\perp}$  represents the intensity of light emitted in the plane perpendicular to the plane of exciting light introduced to the system (Rossi et al.

2011; Souza-Fagundes et al. 2012). The disruption of the FITC-labeled peptide from binding to iASPP results in a change in the amount of polarized light emitted from the system. This assay can be performed in a 96-well or 384-well format and is read on the Envision Multi-label plate reader (Perkin Elmer) (Rossi et al. 2011; Souza-Fagundes et al. 2012).

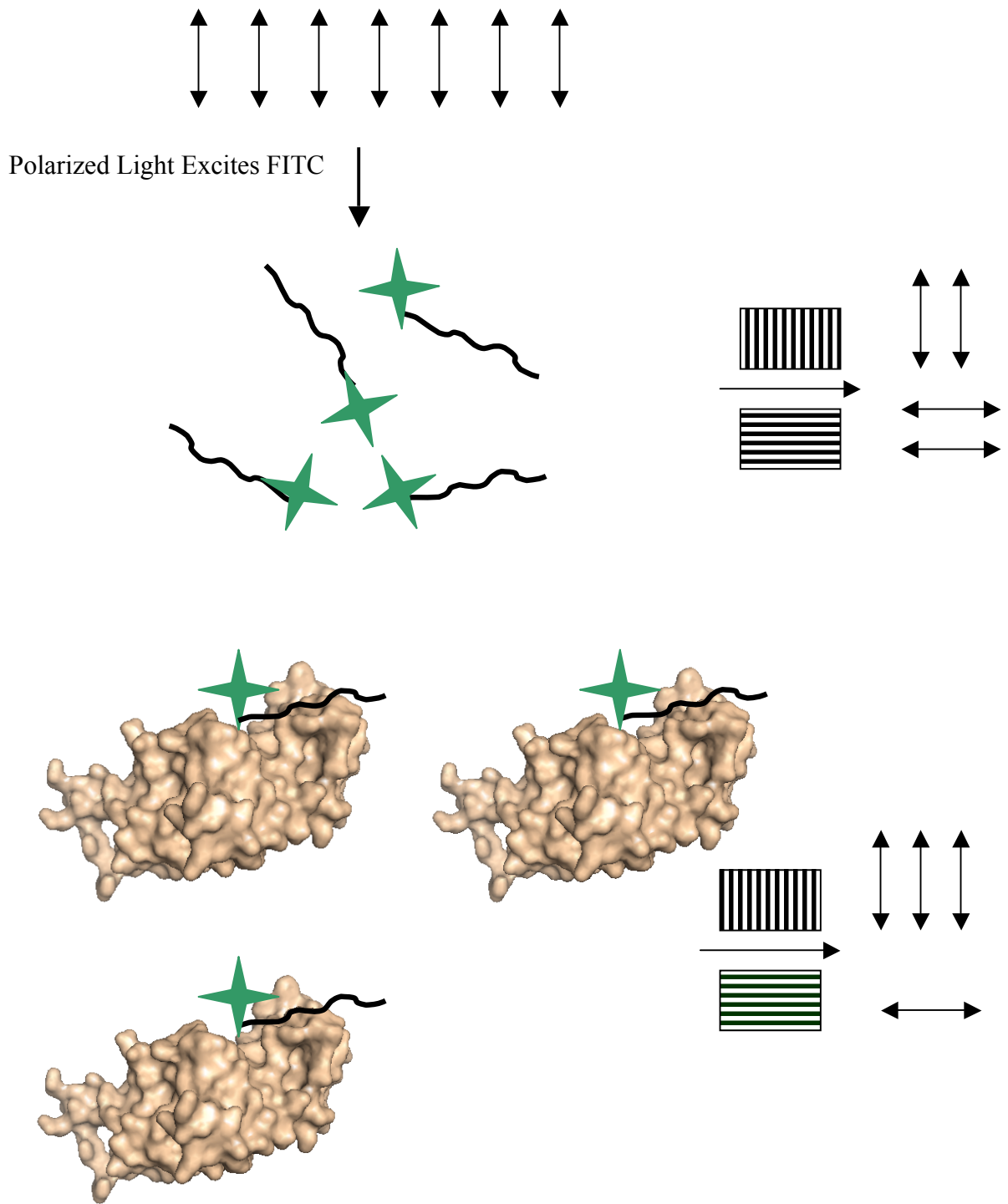


Figure 10. FPA Assay. Green star represents FITC excited by polarized light. The emitted light passed through filters that are parallel and perpendicular to the plane of exciting light. The intensity of light detected in the planes perpendicular and parallel to the exciting light are used to calculate anisotropy.

## Method

Peptides derived from p53 were obtained commercially with and without a FITC probe at the N-terminus. Peptides were re-suspended in water or buffer consisting of 50 mM Tris-HCl, 100 mM NaCl, and 1 mM TCEP or 5 mM BME and stored in aliquots at -20°C. Once aliquots were removed from -20°C, they were diluted to the working concentration of 312 nM and stored at 4°C for up to 48 hours. Several buffer conditions were tested including different concentrations of detergents (Tween 20, NP-40, Triton X) and various salts (100 mM NaCl to 200 NaCl and 100 mM MgCl<sub>2</sub>). The optimal concentration of FITC labeled peptide was examined by testing from 12.5 nM to 250 nM. The final concentration of FITC labeled 9-mer used was 50 nM. Flat bottom black Nunc plates were used for this assay. After the addition of the FITC labeled 9-mer and iASPP, the plate was centrifuged at 1,000 x g for 45 seconds and then rocked at room temperature for 20 minutes prior to reading. The Envision plate reader was used to detect the fluorescence. The raw data was maintained in Excel spreadsheets, and binding affinity calculations and graphs were produced using the Prism software.

## Results

Ideally, the peptides to use for this assay would be derived from an endogenous and biologically relevant binding partner of iASPP. The p53 linker region of iASPP is 34 amino acids in length and has been previously reported to bind to iASPP with an affinity of 16  $\mu$ M (Ahn et al). Because one of our goals is to disrupt the p53-iASPP interaction, the linker region of p53 was used as a starting point for our peptide design. Since, the 34 amino acid p53 linker region is relatively long and could reduce our signal window in

this assay, and is more expensive than shorter peptides we tested seven shorter peptides for use in the FPA assay (Table 6). In addition to the 9 -mer (GSPRKARRA) that has been previously described (Ahn et al, Robinson et al), we designed and tested six additional peptides derived from the p53 linker region. The peptides were designed by first investigating whether the affinity of the p53 linker region was due to either the C- or N-terminus or combinations of the central portion of the peptide. We discovered that both the C-terminus (peptide 2) and the N-terminus (peptide 3) of the p53 linker region have very low affinity for iASPP (Table 6). We also tested the middle region of the p53 (peptides 4-6). For two of the centrally located peptide sequences, we added an arginine residue to either terminus because the 9 -mer as well as the p53 linker region contains a high percentage of arginines and SH3 domains commonly bind to arginine residues. Unfortunately, many of these constructs abrogated binding of the peptides. The only peptides that were found to bind to iASPP were the previously observed 9 -mer (peptide 8), the p53 linker region (peptide 1) and the middle 18 amino acids of the p53 linker region (peptide 7). This is not surprising given that most SH3 domains bind to peptides and proteins containing prolines.



Table 6. Peptide Sequences Investigated for use in FPA assay. \* Indicates a binding affinity established by Ahn et al.

Peptide #	Peptide Sequence	K <sub>d</sub>	Origin
1	LRKKGEPHHELPPGSTKRALPNNTSSSPQPKKKP	16 μM*	p53 linker
2	GSTKRALPNNTSSSPQPKKKP	> 400 mM	p53 linker C-terminus
3	LRKKGEPHHELPPGSTKRAL	> 400 mM	p53 linker N-terminus
4	GSTKRALP	> 400 mM	p53 linker middle 8 mer
5	GSTKRALPR	> 400 mM	p53 linker middle 8-mer + R
6	RSTKRALP	> 400 mM	p53 linker middle 8-mer -G + R
7	EPHHELPPGSTKRALPNN	27 μM	p53 linker middle 18 mer
8	GSPRKARRA	25 μM	iASPP 9-mer

Given these binding affinities, we chose to pursue development of the FPA assay using the p53 linker region (peptide 1) and the 9 -mer (peptide 8). As a first step, we ordered both peptides with an N-terminal FITC moiety. We performed NMR titrations on the FITC -labeled peptides to confirm binding of the modified peptides and to determine the binding affinity. Surprisingly, the affinity of the p53 linker region for iASPP was drastically reduced ( $K_d = 510 \mu\text{M}$ ) upon addition of the FITC label. We concluded that the FITC probe is interfering with binding of the peptide to the protein and is therefore unsuitable for use in this assay.

Therefore, we pursued the development of the FPA assay with the 9 -mer. Determination of the binding affinity of the 9 -mer with and without the FITC label by NMR confirmed the affinity of the labeled peptide (Figure 11).

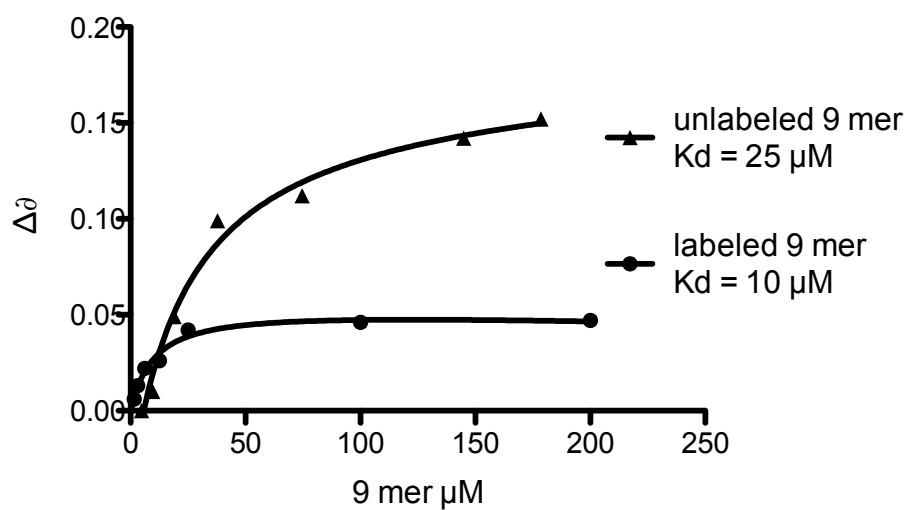


Figure 11. SOFAST-HMQC titration of 9-mer labeled with FITC and unlabeled.  $50 \mu\text{M}$  iASPP in  $50 \text{ mM}$  Tris-HCl,  $100 \text{ mM}$  NaCl,  $1 \text{ mM}$  TCEP, pH 7.3.

Next, we determined the binding affinity of the FITC-labeled 9-mer by our FPA assay as shown in Figure 12.

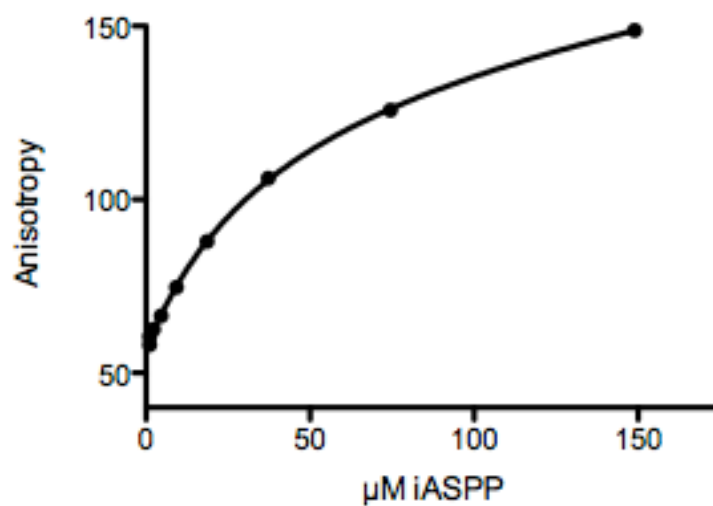


Figure 12. FPA assay iASPP titration for  $K_d$  determination.  $K_d \sim 41 \mu\text{M}$

The difference between the binding affinity of the FITC labeled 9 -mer determined by NMR and by the FPA assay is approximately four fold. Additionally, the binding curve derived from the FPA assay does not plateau and exhibits a linear shape, suggesting this assay is not performing properly. One possible explanation for the observed results could be non-specific binding or aggregation of the peptide. Therefore, we attempted to optimize our assay conditions.

First, we added 1% and 5% DMSO to the FPA assay; this is only difference in conditions between the NMR and FPA assay conditions. However, we saw no improvement of either the binding affinity or of the curve shape upon addition DMSO. Next, we tested different buffer conditions using detergents and salt which can alleviate non-specific interactions. Our initial buffer conditions were 50 mM Tris-HCl, 100 mM NaCl, 1 mM TCEP, pH 7.3. We added detergents at varying concentrations to this buffer including: 1) Tween 20 0.05% 2) Tween 20 0.1% 3) NP-40 0.5% 4) NP-40 0.1% 5) Triton X 0.05% 6) Triton X 0.1%. Then, we experimented with added salt, including: 1) 50 mM MgCl<sub>2</sub> 2) 100 mM MgCl<sub>2</sub> 3) 200 mM NaCl 4) 50 mM MgCl<sub>2</sub> and Tween 20 0.05% 5) 50 mM MgCl<sub>2</sub> and Tween 20 0.1% 6) 50 mM MgCl<sub>2</sub> and NP-40 0.05% 7) 50 mM MgCl<sub>2</sub> and NP-40 0.1% 8) 50 mM MgCl<sub>2</sub> Triton X 0.05% 9) 50 mM MgCl<sub>2</sub> Triton X 0.1%. Figure 13 below shows two of these results. The addition of detergents and salts did not ameliorate the non-specific binding that is adversely affecting our assay.

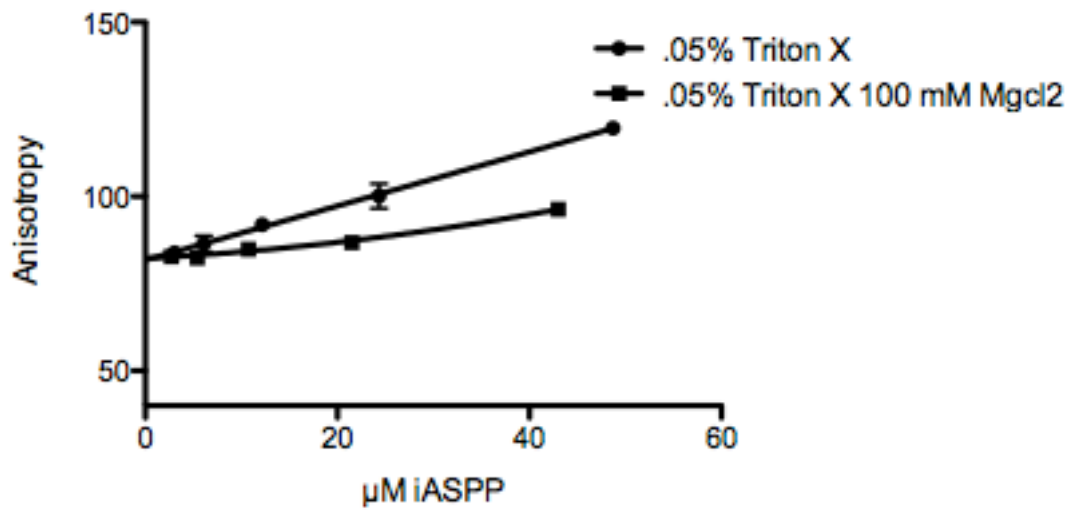


Figure 13. FPA assay binding curve of iASPP and FITC-labeled 9-mer.

Next, we considered whether the unlabeled 9-mer would be able to compete off the FITC labeled 9-mer. This is an important control because it demonstrates that the binding of the FITC labeled 9-mer to iASPP is not due to the FITC probe (Figure 14).

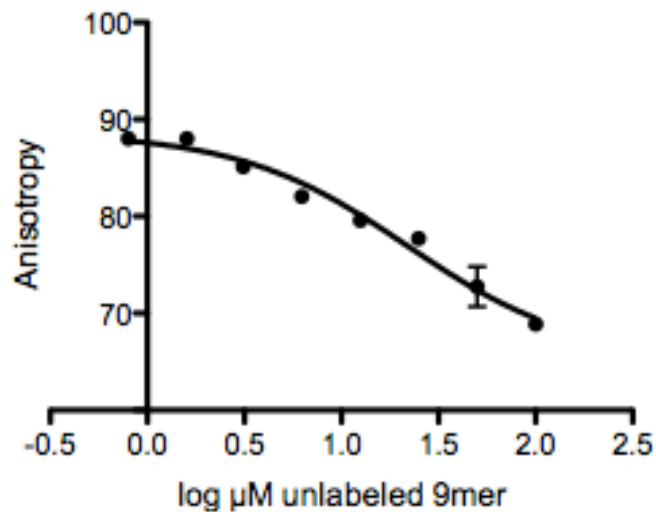


Figure 14. The unlabeled 9-mer competes off FITC labeled 9-mer.

Taken together with the results from our NMR binding studies of the 9 -mer with and without the FITC probe, we conclude that the 9 -mer is binding to our iASPP construct in a manner that is peptide and not FITC probe dependent.

Upon further inspection of the raw data from Figure 12 and repeats (data of repeats not shown), it became apparent that the total fluorescence is decreasing as a function of protein concentration (Figure 15). This is an unexpected result because the total fluorescence should remain the same when the concentration of fluorophore is the same.

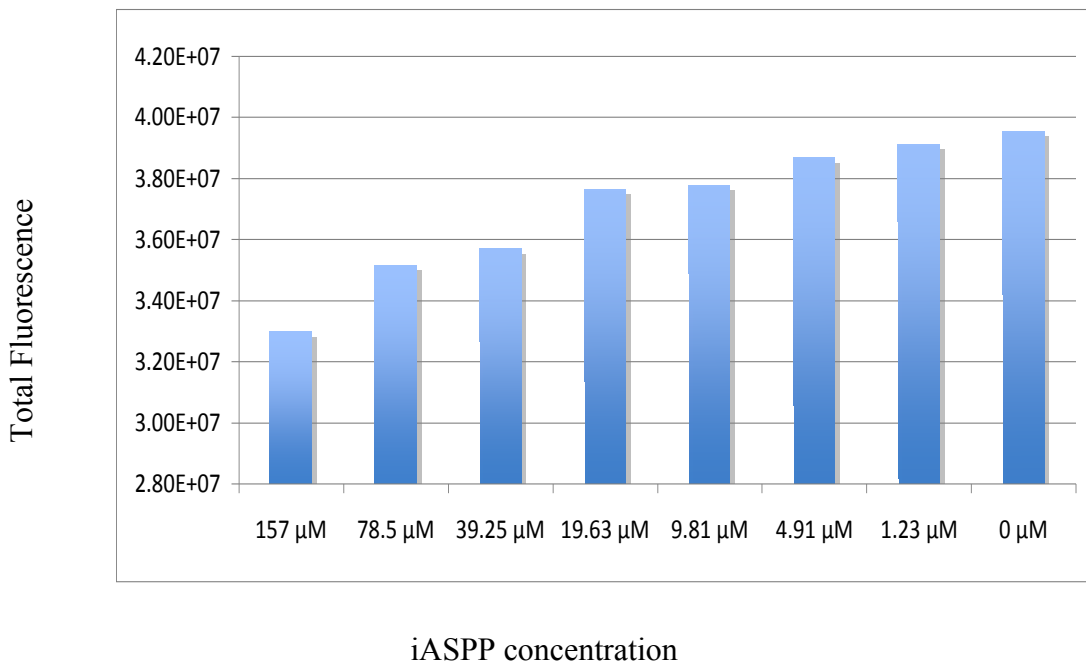


Figure 15. Total fluorescence as a function of iASPP concentration in FPA assay. Total FITC –labeled peptide concentration is constant at 50 nM in all samples.

We hypothesized that binding of the FITC-labeled peptide to iASPP may be responsible for decreasing the total fluorescence. iASPP contains tryptophan residues which are fluorescent and are observed to have an excitation wavelength of 280 nM and an emission wavelength of 348 nM while FITC has an observed absorption wavelength of 495 nM and an emission wavelength of 521 nM. Therefore, it is unlikely that the tryptophan residues are causing the quenching of the FITC probe. If the FITC was quenching upon binding of the peptide to iASPP, we would expect to see this reversal of this effect when the unlabeled 9-mer competes off. However, this was not observed (Figure 16). Therefore, in this case, it seems that FITC should not be used as a fluorescent probe in this assay. Our recommendation to improve this assay would be to

use another fluorescent probe attached to the 9-mer. There are several other fluorescent probes available that would be suitable for this assay including rhodamine derivatives and fluorescein derivatives other than FITC.

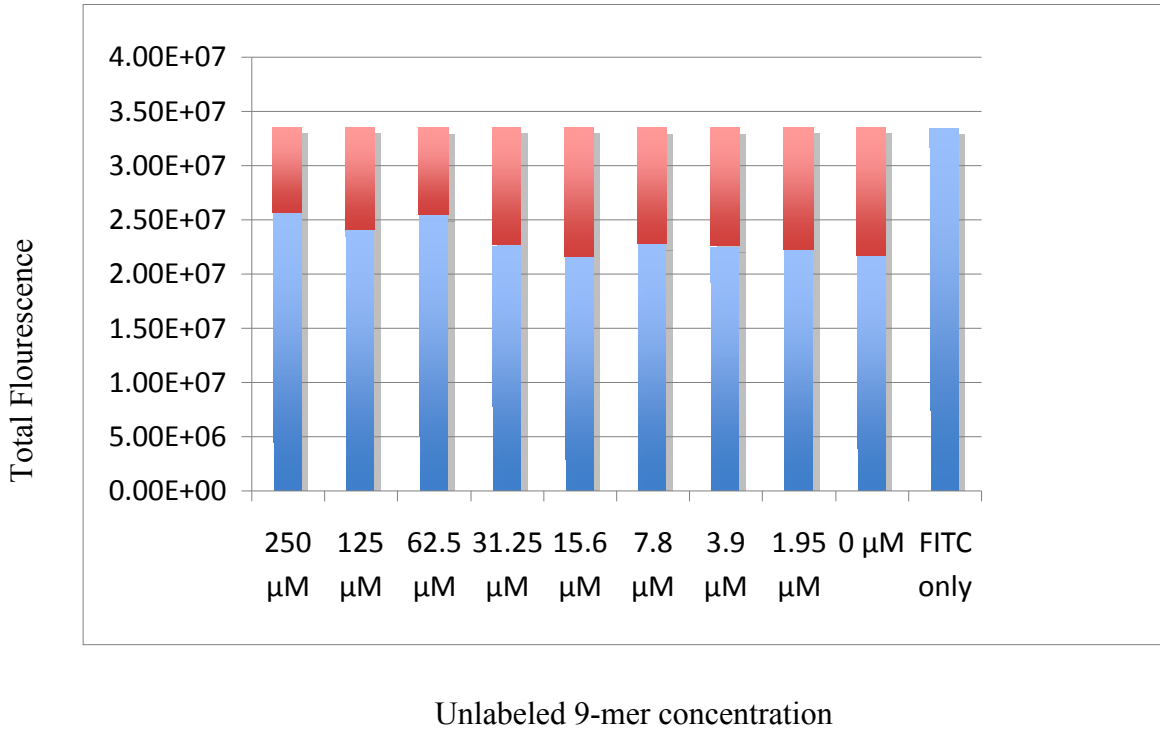


Figure 16. Average total fluorescence values for FP assay where unlabeled 9-mer off-competes the FITC labeled 9-mer. Each concentration of iASPP was measured in triplicate samples. The blue bars indicate the total fluorescence and the red bars indicate the difference between total fluorescence in the FITC only sample when compared to samples containing iASPP.

Alternatively, it may be necessary to develop a different type of assay. One possibility is an ELISA (enzyme linked immunosorbent assay) to observe the disruption of the iASPP-peptide interaction or the iASPP-p53 interaction using full length proteins.



## CHAPTER V

### SUMMARY

The current literature on iASPP suggests that iASPP may be a potential new target for cancer therapy, especially, since iASPP inhibition could potentially initiate apoptosis via p53 or p73 pathways (Bell et al. 2007; Bergamaschi et al. 2003). This is an important advantage because p53 is mutated or deleted in over half of all human tumors (Harms et al. 2004). It is possible to activate apoptosis through p73, which is a part of the p53 family of tumor suppressors and shares many of the same pro-apoptotic targets with p53 (Bell et al. 2007; Bell et al 2008). This makes iASPP an appealing target because we may have the potential to affect apoptosis through not one, but two tumor suppressors in a wide variety of cancers. In addition to inhibiting apoptosis through both p53 and p73, iASPP is over-expressed in several cancer types and is associated with poor response to chemotherapy and metastasis (Liu et al. 2009; Zhang et al. 2005; Jiang et al. 2011; Chen et al. 2012; Li et al. 2011; Lin et al. 2011). Thus far, the reported data on iASPP show that silencing of iASPP in cancer lines and xenograft models is able to reduce proliferation of cancer cells and reduce tumor size (Bell et al. 2007). In addition, studies conducted with a 37 amino acid peptide has shown that disrupting the interaction between p73 and iASPP results in p73- dependent apoptosis in cancer lines with no effect on non-transformed cell lines (Bell et al; 2007).

Because of the apparent function of iASPP in inhibiting apoptosis in many cancer types, we chose to investigate whether iASPP would represent a valuable cancer target. In order to evaluate iASPP as a cancer target, we tested whether it could be druggable with small molecules, whether we could develop biological assays to test binding, and whether we could further validate iASPP as a target in our hands using siRNA.

Once we were able to determine how to prepare enough protein to conduct a fragment-based screen using NMR and optimized the screening conditions, we screened our fragment library containing 15,000 compounds. Several of these small molecules were found to bind to iASPP (hit rate = 0.8%). These results suggest that iASPP is likely to be a druggable protein. Moreover, we were able to identify a few series of compounds that exhibit structure specific binding to iASPP. We measured the binding affinity for many of these fragments and identified fragments that could be used to further develop a small molecule inhibitor to iASPP. Thus, the first criterion in determining if iASPP is a valuable target was met.

Next, we investigated whether a binding assay for iASPP could be developed. These assays are needed to establish whether small molecules are capable of disrupting biologically relevant interactions of iASPP. Towards this end, we attempted to develop a FPA assay. However, we observed a protein-dependent decrease in total fluorescence in our assay. In addition, we found that the binding affinity of the labeled peptide measured in the FPA assay was not in good agreement with the affinity of the labeled peptide

measured by NMR. These data indicate that our FPA assay is not that reliable and thus we abandoned this assay. It might be possible to improve this assay by using a different fluorophore and/or peptide or to develop an antibody-based assay. However, we were unable to validate iASPP as a cancer target using siRNA by experiments conducted by another member of our group, Bhavaratini Vangamundi, as outlined below.

In order to verify and further validate the role of iASPP in cancer cells, Bhavaratini used siRNA to silence iASPP in select cell lines. Seven commercial siRNA motifs (Dharmacon and Santa Cruz) were chosen to silence iASPP. Four of the siRNA constructs resulted in greater than 90% reduction of the protein levels without a corresponding decrease in cancer cell growth or number. This data suggests that perhaps inhibiting iASPP will not have the desired effect. Other groups have reported that iASPP knockdown was accompanied by a selective decrease in cancer cell proliferation (Liu et al. 2009, Liu et al. 2004, Chen et al. 2010). We were able to attain such results with three of the siRNA constructs on particular cell lines. However, one of the constructs that was able to cause a decrease in cancer cell proliferation only reduced protein expression by approximately 80%. These results may be explained by off target effects of the siRNA. Thus, we were unable to correlate protein knockdown with anti-proliferative effects using a number of discrete siRNA motifs against iASPP. Therefore, we did not meet our third criterion in our evaluation of iASPP as a valuable cancer target and decided to stop working on this target to pursue other more promising protein targets in our lab.

## References

- Ahn, J., Byeon, I., Byeon, C., Gronenborn, A. 2009. Insight into the Structural Basis of Pro- and Antiapoptotic p53 modulation byASPP proteins. *J. Biol Chem.* 284: 13812-13822.
- Baker. L. Quilen, P., Patten, N., Ashfield, A., Birse-Stewart-Bell, L., McCowen, C., Bourdon, J., Purdie, A., Jordan, L., Dewar, A., Wu, L., Thompson, A. p53 mutation, deprivation and poor prognosis in primary breast cancer. 2010. *B J Cancer.* 102:719-726.
- Bell, H. Dufes, C., O'Prey, Crighton, D., Bergamaschi, D., Lu, X., Schatzlein, A., Vousden, K., Ryan, K. 2007. A p53-derived apoptotic peptide derepresses p73 to cause tumor regression *in vivo*. *J. Clin. Inv.* 117: 1008-1018.
- Bell, H and Ryan, K. 2008. iASPP Inhibition: Increased Options in Targeting the p53 Family for Cancer Therapy. *Cancer Res.* 68: 4959-4961
- Bell, H and Ryan, K. Targeting the p53 Family for Cancer Therapy: 'Big Brother' Joins the Fight. 2007. *Cell Cycle.* 6: 1995-2000.
- Bergamaschi, D., Samuels, Y. O'Neil, N., Trigiante, G., Crook, T., Hseih, J., O'Connor, D., Zhong, S., Campargue, I., Tomlinson, M., Kuwabara, P., Lu, X. 2003. iASPP oncoprotein is a key inhibitor of p53 conserved from worm to human. *Nat. Gen.* 33: 162-167.
- Canning, P., von Delft, F. Bullock, A. 2012. Structural basis for ASPP2 recognition by the tumor suppressor p73. *J. Mol. Biol. Epub.* 2012 Aug 20.
- Chen, J., Xie, F., Zhang, L., Wen, J. 2012. iASPP is over-expressed in human non-small cell lung cancer and regulates the proliferation of lung cancer cells through a p53 associated pathway. *BMC Cancer.* 10: 694.
- Deng, Q., Sheng, L. Su, D., Zhang, L., Liu, P., Lu, K., Ma, S. Genetic polymorphisms in ATM, ERCC1, APE1 and iASPP genes and lung cancer risk in a population of southeast China. 2010. *Med. Oncol.* 28: 667-672.
- Gillotin, S. 2009. iASPP, A potential drug target in cancer therapy. *Leuk. Res.* 33: 1175-1177.
- Gorina, S., Pavletich, N. 1997. Structure of the p53 tumor suppressor bound to the ankyrin and SH3 domains of 53BP2. *Science.* 8: 1001-1005.
- Hajduk, P., Greer, J. 2007. A decade of fragment-based drug design: strategic advances and lessons learned. *Nat Rev Drug Disc.* 6: 211-219.

- Harms, K., Nozell, S., and Chen, X. 2004. The common and distinct targets of the p53 family of transcription factors. *Cell Mol. Life Sci.* 61: 822-842.
- Jiang, L., Siu, M., Wong, O., Tam, K., Lu, X., Lam, E., Ngan, H., Le, X., Wong, E., Monteiro, L., Chan, H., Cheung, A. 2011. iASPP and chemoresistance in ovarian cancers: effects on paclitaxel mediated mitotic catastrophe. *Clin Cancer Res.* 17: 6924-6933.
- Lin, B., Xie, D., Xie, S., Zhang, X., Zhang, Y., Gao, Z. 2011. Down-regulation of iASPP in human heptaocellular carcinoma cells inhibits cell proliferation and tumor growth. *Neoplasma.* 58: 205-210.
- Liu, H., Wang, M., Diao, S., Rao, Q., Zhang, X., Xing, H., Wang, J. siRNA-mediated down-regulation of iASPP promotes apoptosis induced by etoposide and daunorubicin in leukemia cells expressing wild-type p53. 2009. *Leuk. Res.* 33: 1243-1248.
- Liu, Z., Zhang, Y., Zhang, X., Yang, X. 2004. Abnormal mRNA expression of ASPP members in leukemia cell lines. *Leukemia.* 18: 880.
- Menendez, D., Inga, A., Resnick, M. 2009. The expanding universe of p53 targets. *Nat. Rev. Cancer.* 9: 724-737.
- Robinson, R., Lu, X., Jones, E., Siebold, C. 2008. Biochemical and structural studies of ASPP proteins reveal differential binding to p53, p63, and p73. *Structure.* 16: 259-268.
- Rossi, A., Taylor, C. 2011. Analysis of protein-ligand interactions by fluorescence polarization. *Nat. Protoc.* 6: 365-387.
- Schanda, P., Kupce, E., Brutscher, B. 2005. SOFAST-HMQC experiments for recording two-dimensional heteronuclear correlation spectra of proteins within a few seconds. *J. Biomol. NMR.* 33: 199-211.
- Shuker, S., Hajduk, P., Meadows, R., Fesik, S. 1996. Discovering High-Affinity Ligands for Proteins: SAR by NMR. *Science.* 274: 1531-1534.
- Souza-Fagundes, E., Frank, A., Feldkamp, M., Dorset, D., Chazin, W., Rossanese, O., Olejniczak, E., Fesik, S. 2012. A high-throughput fluorescence polarization assay for the 70N domain of replication protein A. *Anal. Biochem.* 421: 742-749.
- Su, D., Ma, S., Liu, P., Jiang, Z., Lv, W., Zhang, Y., Deng, Q., Smith, S., Yu, H. 2007. Genetic polymorphisms and treatment response in advanced non-small cell lung cancer. *Lung Cancer.* 57: 281-288.

- Sullivan, A. and Lu, X. ASPP: a new family of oncogenes and tumor suppressor genes. 2007. *B J Cancer*. 96:196-200.
- Vigneron, A., Ludwig, R., Vousden, K. 2010. Cytoplasmic ASPP1 inhibits apoptosis through the control of YAP. *Genes Dev*. 24: 2430-24309.
- Zhang, X, Wang, M., Zhou, C., Chen, S., Wang, J. 2005. The expression of iASPP in acute leukemias. *Leuk. Res*. 29: 179-183.
- Zhang, B., Xiao, H., Chen, J., Tao, J., Cai, L. 2011. Inhibitory member of the apoptosis stimulating protein of p53 (ASPP) family promotes growth and tumorigenesis in human p53-deficient prostate cancer cells. *Prostate Cancer Prostatic Dis*. 14: 219-224.